VLA synthesis of H I absorption toward SGR A

Liszt, H.S.; Hulst, J.M. van der; Burton, W.B.; Ondrechen, M.P.

Astron. Astrophys. 126, 341–351 (1983)

ASTRONOMY AND ASTROPHYSICS

VLA synthesis of H I absorption toward Sgr A

H. S. Liszt[1], J. M. van der Hulst[2], W. B. Burton[3], and M. P. Ondrechen[4]

[1] National Radio Astronomy Observatory, Edgemont Road, Charlottesville, VA 22901, USA
[2] Netherlands Foundation for Radio Astronomy, Radiosterrenwacht Westerbork, Schattenberg 4, 9433 TA Zwiggelte, The Netherlands
[3] Sterrewacht Leiden, Postbus 9513, 2300 RA Leiden, The Netherlands
[4] Department of Astronomy, University of Minnesota, 116 Church Street, S.E., Minneapolis, MN 55455, USA

Received November 8, 1982; accepted June 8, 1983

Summary. We have synthesized H I absorption against Sgr A using the VLA with 12″ angular resolution and 6 km s^{-1} velocity resolution over the range $-300\,\mathrm{km\,s^{-1}} \lesssim v \lesssim 250\,\mathrm{km\,s^{-1}}$. To support the analysis of these observations we have also observed ^{12}CO emission on a 45″ grid near Sgr A using the 36-foot NRAO telescope on Kitt Peak. H I absorption features are found at all velocities in the range $-200\,\mathrm{km\,s^{-1}} \leqq v \leqq 140\,\mathrm{km\,s^{-1}}$, i.e., over almost the entire interval prominent in ^{12}CO emission near $l=0°$, $b=0°$. Apparently, the emitting gas at $v>150\,\mathrm{km\,s^{-1}}$ lies exclusively beyond the Sgr A continuum, because at other velocities the H I optical depth and ^{12}CO brightness temperature peaks coincide. Such similarity in the two species shows that column density variations must determine the optical depth patterns in the H I absorption, most of which arises in cool, dense molecular clouds with a small proportion of residual atomic hydrogen. Although it avoids nearly all the thermal flux from Sgr A (West), gas at 40–60 km s^{-1} does absorb against the compact source, indicating that both the East and West continuum components lie behind this gas. The gas cloud at $-190\,\mathrm{km\,s^{-1}}$ is narrowly confined at negative longitudes and extended $\geqq 3'$ in latitude.

Key words: galactic center – H I regions – interstellar clouds – molecular clouds – interstellar absorption

I. Introduction

The line of sight to the Sgr A continuum complex has been the subject of many absorption studies; some of the most anomalous aspects of galactic kinematics were first found in such work – the outwardly-directed motion of the 3 kpc arm at $-53\,\mathrm{km\,s^{-1}}$ (van Woerden et al., 1957; Rougoor and Oort, 1960; Rougoor, 1964), the existence and outwardly-directed motion of the $-135\,\mathrm{km\,s^{-1}}$ "expanding molecular ring" feature (Scoville, 1972), and the presence of absorbing gas in the direction of the Sgr A complex at a range of positive velocities (e.g. Sandqvist, 1970) are prominent examples. Absorption-line spectra taken toward Sgr A have been used to constrain the space motion of the Local Standard of Rest and the kinematics of gas in the galactic disk (e.g. Kerr and Westerhout, 1965), and to determine the geometry of the radio-continuum sources in the nucleus itself (Whiteoak et al., 1974). More recently, Güsten and Downes (1981) have identified a new feature at $-190\,\mathrm{km\,s^{-1}}$ in H I and H_2CO absorption profiles taken in the vicinity of Sgr A and Linke, Stark, and Frerking (1981) detected a broad negative-velocity feature in HCO^+ and HCN at λ 3 mm, confirming the extraordinarily high gas masses ($>10^9\,M_\odot$) inferred to lie in the inner $\sim$3 kpc by Liszt and Burton (1978).

The structure of Sgr A has itself been the subject of much recent work at infrared and radio wavelengths, with observations of the 12.8 μ Ne II line of particular interest because they have yielded information at high spatial resolution on both the distribution and kinematics of the thermally-emitting gas flows in the nucleus (Lacy et al., 1979, 1980). Radio-continuum measurements with the VLA have begun to clarify the morphology of the Sgr A (East) and (West) components (Brown et al., 1981; Ekers et al., 1983). The non-thermal compact source in (West) is superposed on, and probably embedded in, a multi-trunked thermally emitting structure whose kinematics can be observed either in the Ne II transition or in cm-wave recombination lines (van Gorkom et al., 1983). The non-thermal source Sgr A (East) is actually part of a full shell-structure which passes through (West) as seen on the sky, contributing some non-thermal flux even toward the thermal-emission regions. Taken together, these results indicate that the thermal emission in (West) emanates from (or is somewhat tied to) the compact source and that (East) and (West) are possibly physically associated or co-located. Interpretation of absorption line data, on the other hand, has usually yielded the conclusion that (East) and (West) are separated by a neutral gas cloud at 40–60 km s^{-1}; reconciliation of the absorption-line data with the newly inferred source structure represents the main motivation for undertaking the work reported here.

Use of the VLA to measure absorption spectra toward Sgr A offers both higher spatial resolution and wider velocity coverage than previously available. Here, we present synthesis maps of the H I absorption against both (East) and (West) at 12″ angular resolution (corresponding to 0.6 pc at a distance of 10 kpc), covering a velocity range $-300\,\mathrm{km\,s^{-1}} \lesssim v \lesssim 250\,\mathrm{km\,s^{-1}}$ with 6 km s^{-1} spectral resolution. To aid in the interpretation of these data, we also present new ^{12}CO emission maps taken over a $5' \times 5'$ region around Sgr A with 45″ spacings of the 66″ beam of the 36-foot telescope on Kitt Peak. We found the molecular emission data crucial in interpreting the observed absorption patterns because of its ability to detect column density variations independent of location of the gas with respect to the galactic center. Although absorption lines provide unambiguous determination of the placement of the gas relative to the background source if they are seen, they cannot by themselves allow distinction between variations in column density or temperature, nor do they allow distinction of such variations from a space distribution in which the gas is present but passes behind the background continuum source (Liszt et al., 1975).

Send offprint requests to: W. B. Burton

We show here that there is a good correspondence between the H I and CO kinematics and morphology which implies: 1. that the H I absorption arises in most cases in molecular clouds; 2. that the observable absorption patterns are manifestations of column-density variations (rather than resulting from a disposition of the gas which places it behind some continuum sources and in front of others); and 3. that the distribution of the CO gas toward Sgr A is very asymmetrical, most lying closer to the Sun than Sgr A itself. Our spatial resolution is high enough that we can obtain spectra against the compact source separately and we show that the $+50\,\mathrm{km\,s^{-1}}$ cloud, previously supposed not to occult any portion of (West), is detectable in absorption in this direction. The gas cloud at $-190\,\mathrm{km\,s^{-1}}$ recently discovered by Güsten and Downes (1981) occurs mainly in a narrow ridge at longitudes below that of the compact source but extends several arcminutes in latitude.

II. Observations

a) H I *absorption synthesis observations at the* VLA

Our observations at the VLA were made on 1981 26–27 May using 9 antennae in the 10 km configuration (for a complete description of the VLA see Thompson et al., 1980) and a

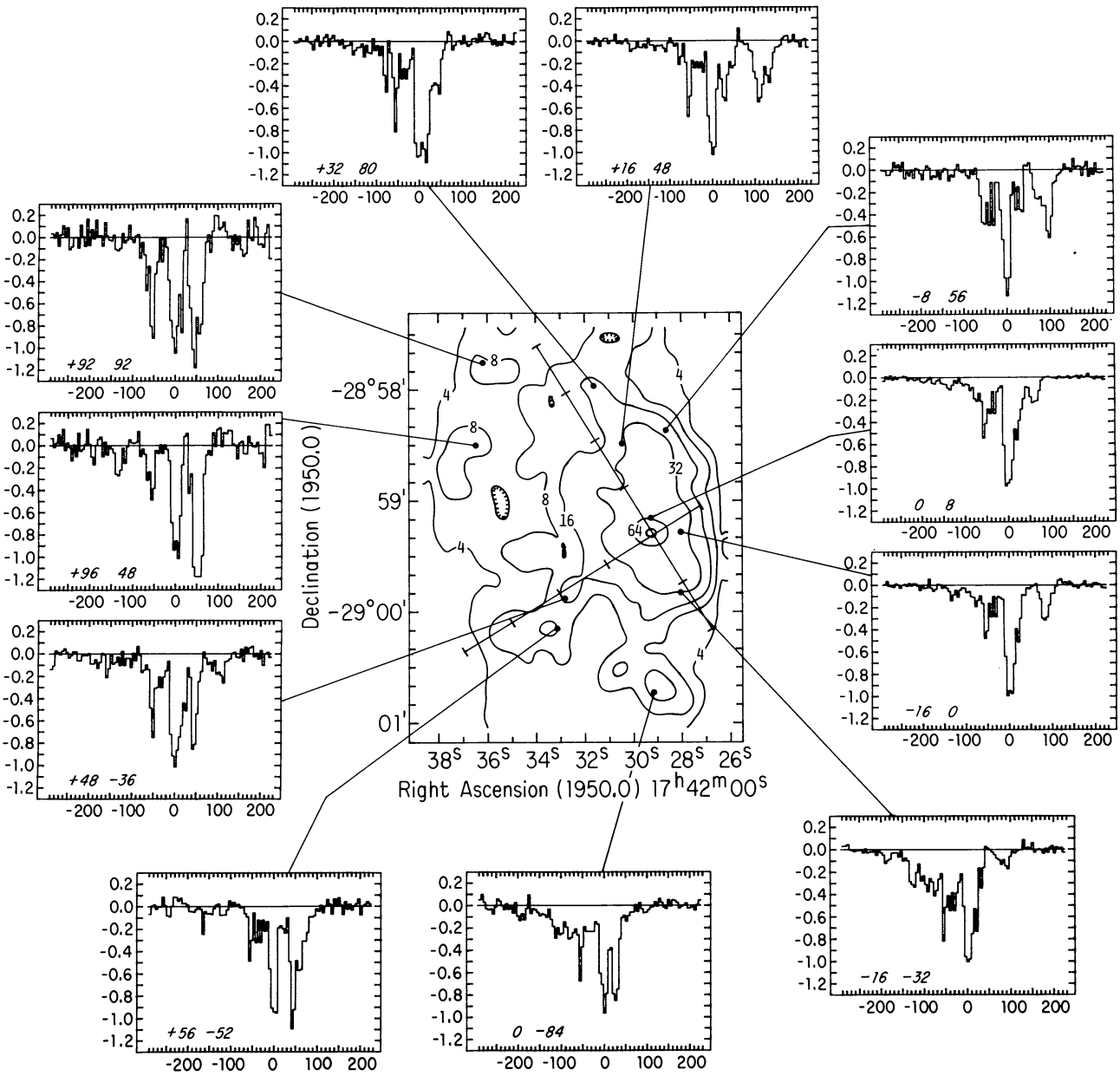

Fig. 1a. The Sgr A pseudo-continuum map and representative H I absorption spectra. Continuum contour levels are shown at 4%, 8%, 16%, 32%, 64%, and 96% of the peak, ~2.4 Jy/beam: all H I maps shown have been restored with a 12″ (FWHM) circular Gaussian. The absorption spectra, in the form (line/continuum) − 1, are labelled with r.a.-dec offsets (in arcseconds) from the position of the compact source at r.a.(1950) = $17^h42^m29^s.3$, dec(1950) = $-28°59'18''.6$. Velocities are measured with respect to the Local Standard of Rest and the channel spacing is $5.16\,\mathrm{km\,s^{-1}}$. Superimposed on the continuum is a cross in galactic co-ordinates, centered on the compact source, with tics at 30″ intervals

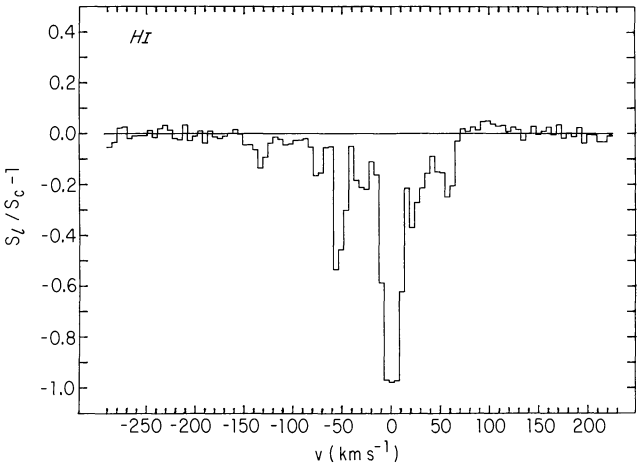

Fig. 1b. H I absorption toward the compact source in Sgr A (West). This spectrum was obtained in a separate 3^h coherent integration with angular resolution 3″ as described in Sect. II of the text. Only phase and bandpass calibration (i.e. no "CLEAN"ing or other such post-processing) were used to produce this spectrum. A linear baseline amounting to 0.01 in optical depth across the band has been subtracted

3.125 MHz bandwidth ($\approx 660\,\mathrm{km\,s^{-1}}$) of 128 channels, each of width $6.2\,\mathrm{km\,s^{-1}}$ spaced by $5.16\,\mathrm{km\,s^{-1}}$. On the first night, we made a long (3^h) coherent integration using antennae at the end of each arm and discarding intra-arm antenna pairs in order to sample flux from the compact source while filtering out the broader ($\geqq 3''$) spatial structures of Sgr A. It was in these data that the $+50\,\mathrm{km\,s^{-1}}$ gas was found toward (West) and the spectrum obtained in this way is shown in Fig. 1 to corroborate the results of our mapping, which necessarily entails a far higher degree of processing of the raw visibilities. This spectrum has had the usual phase and bandpass calibration, but is un-"CLEANED". On the second night we used 9 antennae spaced more evenly throughout the array and got 3^h of on-source integration interspersed with observations of phase and bandpass calibrators. The phase calibration so obtained was insufficient and caused the appearance of many spurious emission features with unrealistically high brightness temperatures ($\gg 10^3$ K). After discovering the poor phase calibration, the data were set aside until 1982 April when the use of Schwab's (1980) method and his assistance made it possible to self-calibrate the line data using the compact source as a reference. Self-calibration phase corrections were determined iteratively for the continuum emission composed of the (absorption-free) outermost channels. These corrections were applied to the uv data for the remaining 100 channels containing the H I absorption. Maps of the line channels were then differenced with the (self-calibrated) continuum and the difference maps were "CLEANED" and divided by the "CLEAN" continuum map to provide the absorption spectra. The observations were tapered in the uv plane to yield a 12″ circular beam.

After self-calibration the absorption spectra were found to be free of the spurious emission found previously, but one slight problem does remain. Toward Sgr A (East) the line flux in the $50\,\mathrm{km\,s^{-1}}$ gas is slightly negative relative to the zero level established by the absorption-free (but not flux-free) channels at the band edge. Such pseudo-absorption can arise in the presence of a strongly absorbing line whose sharply varying spatial structure is very different from that of the underlying continuum (and in the presence of inadequate sampling of the uv plane), but it cannot occur where deep absorptions do not exist. We have in any case truncated all derived optical depths at 4. The $50\,\mathrm{km\,s^{-1}}$ cloud is known to be strongly saturated toward (East) with even larger opacities in some places according to Schwarz et al. (1982), and the maps presented below should not suffer any serious distortion. Uncertainties in the H I absorption column density arise from indeterminacy of the spin temperature and it would be impossible to provide an accurate value for N_{HI} even if the opacity were better known. In most cases, the H I opacities arise in cold dense clouds for which $N_{\mathrm{HI}} \ll H_{\mathrm{H_2}}$ anyway.

The final dataset has an rms noise ~ 18 mJy (per channel per beam) or ~ 81 K at 12″ resolution; the continuum flux raises the system temperature by a factor ~ 3 and we have not determined a precise flux scale because of our interest in absorption spectra. At the field center (that of the compact source given by Brown et al., 1981: $\alpha(1950) = 17^h42^m29^s.335$, $\delta(1950) = -28°\,59'\,18''.6$) the detected flux is ~ 2.4 Jy/beam and the rms error in τ is $\leqq 1\%$. The maps are presented in the figures discussed below for the regions where the flux is above $\sim 7\%$ of the peak. The noise level in the general run of spectra can be examined in Fig. 1.

b) CO emission observations at the 36-foot telescope

The CO observations were taken at the NRAO 36-foot telescope on Kitt Peak on 1982 May 12–13. At λ 2.6 mm the telescope beam main lobe is 66″ in diameter. The channel spacing was 1 MHz or $2.6\,\mathrm{km\,s^{-1}}$. The observations were made at 45″ spacings on a $\sim 5' \times 5'$ grid centered just ($\sim 20''$) north of the compact source. The intensity scale is $T_A^*/0.65$, the radiation temperature for a 65% beam efficiency (in accord with our earlier work).

III. H I absorption toward Sgr A

In Fig. 1 we show a few spectra taken at representative positions across Sgr A. The continuum emission does not show the full shell-structure of which Sgr A (East) is a part (Ekers et al., 1983) nor are the thermal structures found near the compact source in evidence. The latter situation arises because of low spatial resolution and the dominance of non-thermal emission at $\lambda \sim 21$ cm, the former because our observations did not involve antenna spacings sufficiently short to provide full information on the extended shell structure.

The absorbing gas is comprised of many velocity features with a wide variety of behaviour, some of which can be seen by examining the representative spectra in Fig. 1:

1. There are absorption features at velocities as high as $+135\,\mathrm{km\,s^{-1}}$ ($\Delta\alpha = 16''$, $\Delta\delta = 48''$) and as low as $-190\,\mathrm{km\,s^{-1}}$ ($-16''$, $-32''$). This negative velocity gas was first discussed by Güsten and Downes (1981) and is shown below to occur mainly at negative longitudes (all longitudes Δl and latitudes Δb discussed here are measured relative to the compact source position). The $+100\,\mathrm{km\,s^{-1}}$ feature seen below and to the north of the compact source appears as a weak wing in single-dish H_2CO profiles of Güsten and Downes (1981) but no previous H I spectra have found absorption at $v \gtrsim 70\,\mathrm{km\,s^{-1}}$ (see Schwarz et al., 1982).

2. The cloud centered at $+50\,\mathrm{km\,s^{-1}}$ is strong in the eastern portion of the map. It weakens closer to the compact source but does not entirely disappear there. At the western edge of the map there is a prominent absorption feature at $\sim 90\,\mathrm{km\,s^{-1}}$.

3. A new feature at $-75\,\mathrm{km\,s^{-1}}$ is seen to the north ($+32''$, $+80''$) of the compact source.

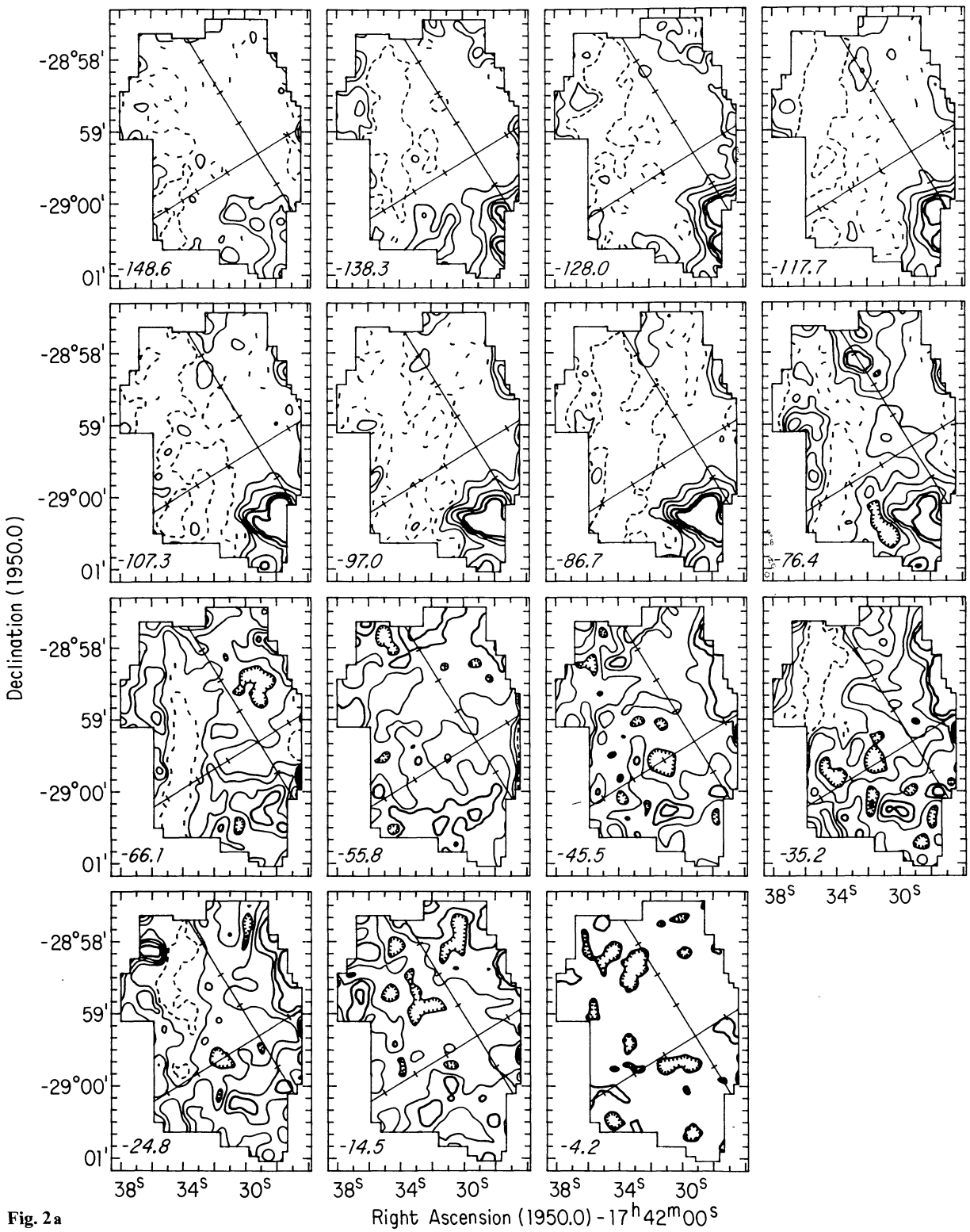

Fig. 2a

Fig. 2. H I optical depth maps. The optical depth has been summed over 3 channels (15.5 km s^{-1}) centered at the velocity indicated in the lower left-hand corner of each panel. Shown are contours at $\int \tau dv = 0$ km s^{-1} (dashed) 2, 4, 8, 16 (bold), 32 (bold) km s^{-1}. Note the presence of absorption from the ~ 50 km s^{-1} gas toward the compact continuum source in Sgr A (West)

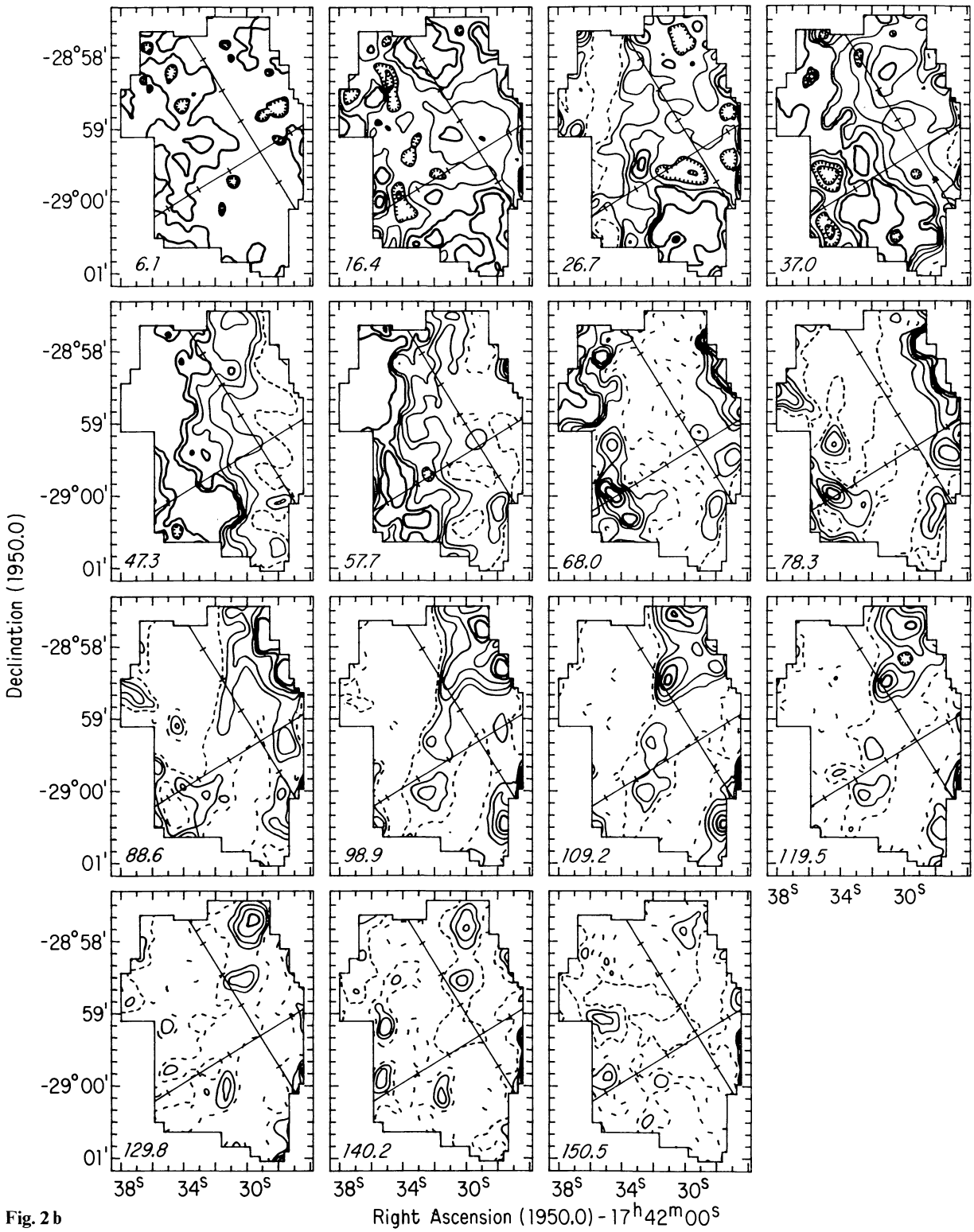

Fig. 2 b

4. In the region $\Delta l<0'$ there is a very broad negative velocity wing on the absorption spectra, extending from $\sim -30\,\mathrm{km\,s^{-1}}$ to $\lesssim -150\,\mathrm{km\,s^{-1}}$. This wing is present in some H_2CO profiles of Güsten and Downes (1981) and can be mapped in CO (see Sect. IV below).

Maps of optical depth integrated over 3 channels, $\sim 16\,\mathrm{km\,s^{-1}}$, and spaced by 2 channels, $10\,\mathrm{km\,s^{-1}}$, are shown in Fig. 2; an integrated opacity of $1\,\mathrm{km\,s^{-1}}$ corresponds to an absorption column density $N_{\mathrm{HI}} = 1.8\,10^{18}\,(T_{\mathrm{spin}})\,\mathrm{cm^{-2}}$. The most conspicuous structure at negative velocities occupies a small region at $\Delta l \sim -45'$ spanning most or all of the range $v \lesssim -70\,\mathrm{km\,s^{-1}}$ as noted in the discussion of Fig. 1. Where it occurs, the absorption from both the $-135\,\mathrm{km\,s^{-1}}$ feature and from the 3 kpc arm at $-53\,\mathrm{km\,s^{-1}}$ are enhanced. The origin of such a broad but localized feature is unclear, but, as shown utilizing CO spectra in the next section, there is a high column density gas associated with it. It is not the case, for example, that an extraneous background source is present causing the absorption column length to increase. This feature occurs at the edge of our continuum map, and neither the main body of Sgr A (West) nor the clump at $\Delta\alpha \approx 0'$, $\Delta\delta \approx -80'$ (part of the non-thermal shell structure) underlies it.

Many other features are present at negative velocities, but in general, these arise from structures extending many degrees around the center. The 3 kpc arm shows variations of a factor $\sim$two in opacity, at least partly due to its superposition in velocity with other gas. Menon and Ciotti (1970) have observed emission from the $-25\,\mathrm{km\,s^{-1}}$ gas at $l \sim -350° \rightarrow 5°$.

The behaviour of the gas at positive velocities is more diverse and has given rise to some controversy. At $16.4\,\mathrm{km\,s^{-1}}$ in Fig. 2 the disposition of the absorption on either side of (West) has been noted previously in H_2CO (Whiteoak et al., 1974). A $\sim 20\,\mathrm{km\,s^{-1}}$ cloud extends to $l \sim -0.^{\circ}2$ in the maps of Güsten and Downes (1980) but maps of ^{12}CO show prominent emission over several degrees (Liszt and Burton, 1978), the closest peaks to Sgr A occurring at $\Delta l \approx +600'$ and $-240'$. At higher ($20\,\mathrm{km\,s^{-1}} < v < 70\,\mathrm{km\,s^{-1}}$) velocities, the absorption lines shift progressively to higher longitude and lower latitude, with much of the eastern portion of the non-thermal shell-structure covered by high optical depth gas. One characteristic not disclosed by earlier synthesis observations is that a small tongue of gas occults the compact source at velocities up to $\sim 60\,\mathrm{km\,s^{-1}}$ – as the main body of gas shifts away from the direction of (West) ($v = 47, 57\,\mathrm{km\,s^{-1}}$ in Fig. 2) a fragment is left behind. This fragment has a noticeable shift in position with velocity but is clearly part of the gas which dominates the absorption of Sgr A (East).

The gas at 40–60 $\mathrm{km\,s^{-1}}$ has been supposed not to occult Sgr A (West) and has been inferred, as a result, to lie between (East) and (West) (Whiteoak et al., 1974; Oort, 1974). It was argued somewhat later that strong column density variations render this inference unreliable (Liszt et al., 1975); our H I spectra and recent information concerning the continuum structure support this argument. The earlier geometrical reconstruction, if applied to our data, would imply that the compact source is removed behind most of (West). However, the thermal emission in (West) which is not absorbed clearly emanates from the position of this source (Brown et al., 1981; Ekers et al., 1982). It is also known that the non-thermal shell passes through the direction of (West) and, if it were covered uniformly at high opacity, absorption would be present weakly but ubiquitously over (West). Such a situation is not observed.

At velocities $\sim 70\,\mathrm{km\,s^{-1}}$, absorption brackets Sgr A (West), a spatial pattern also seen by Schwarz et al. (1982). At $\Delta l<0'$ this absorption is due to the high velocity wing of the $50\,\mathrm{km\,s^{-1}}$ cloud. At still higher velocities, clouds are seen chiefly at $\Delta l>0'$. As indicated in Fig. 1, features are present with center velocities up to $+135\,\mathrm{km\,s^{-1}}$ but no absorption is detected at $v \gtrsim 150\,\mathrm{km\,s^{-1}}$.

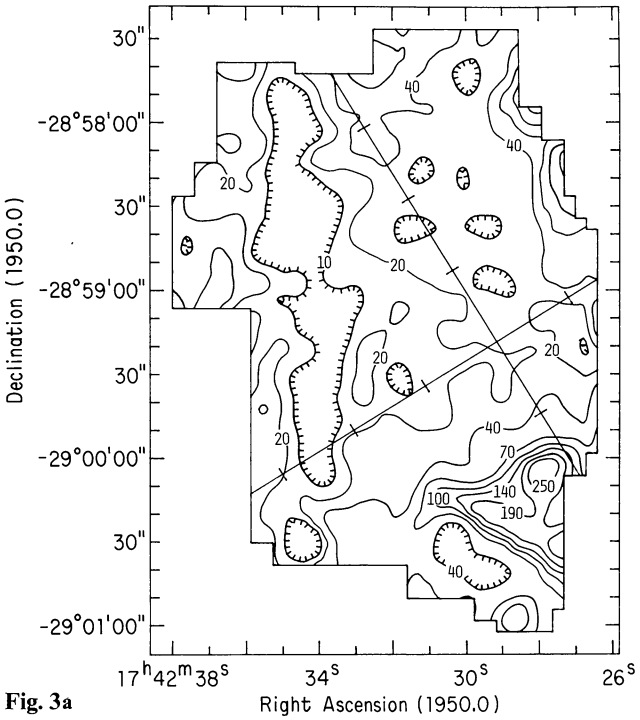

Fig. 3a

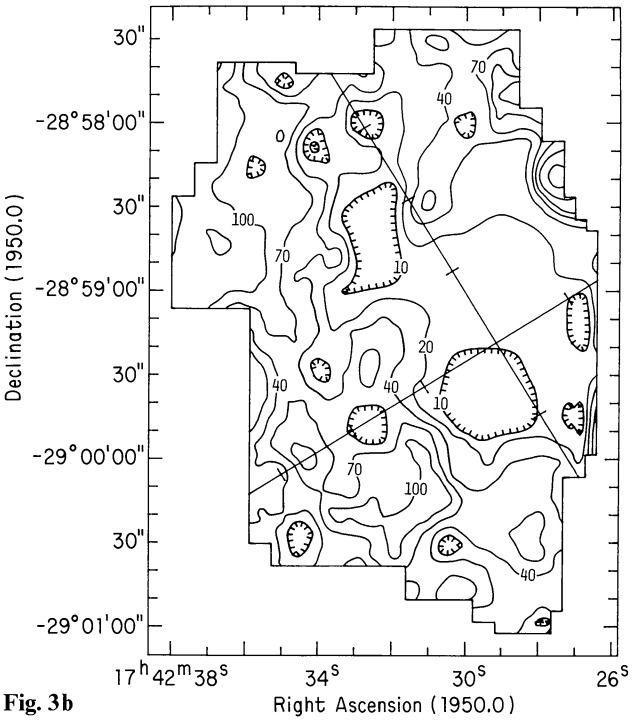

Fig. 3b

Fig. 3a–c. H I optical depth maps integrated over wide velocity ranges. Units are $\mathrm{km\,s^{-1}}$. **a** for $-150 \leqq v \leqq -15\,\mathrm{km\,s^{-1}}$, **b** for $+15 \leqq v \leqq +150\,\mathrm{km\,s^{-1}}$, **c** for $15\,\mathrm{km\,s^{-1}} \leqq |v| \leqq 150\,\mathrm{km\,s^{-1}}$

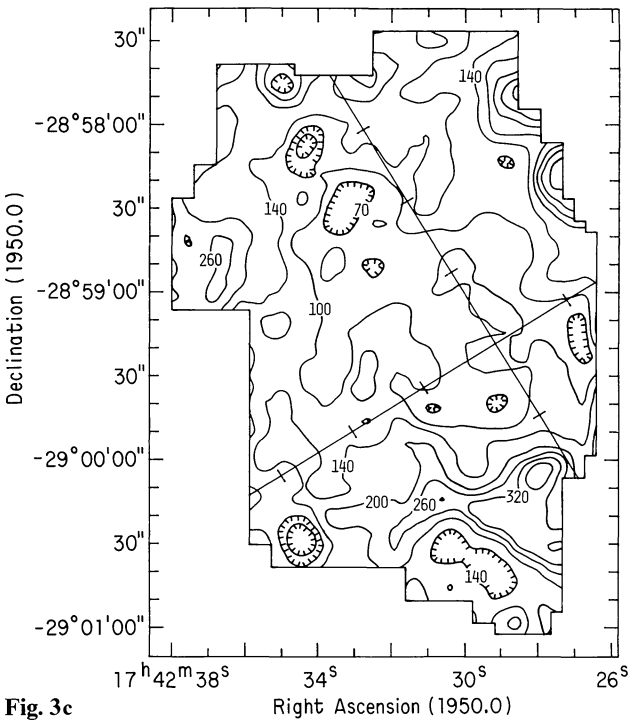

Fig. 3c

We summarize these remarks by noting that the distribution of the absorbing gas is a) asymmetrical in the sense that nearly all the features visible in emission in ^{12}CO toward $\Delta l \sim 0'$ lie at least partly in front of Sgr A (see Fig. 1a of Liszt and Burton, 1978), b) but that it is not dominated by a single, general rotational velocity gradient, even though the highest negative velocities do occur at $\Delta l < 0'$ and the highest positive velocities at $\Delta l > 0'$, and c) it is generally displaced from (West).

The latter two points are illustrated by maps of opacity integrated over negative and positive velocities shown in Fig. 3. Neither positive- or negative-velocity gas occurs exclusively on one side of $\Delta l = 0''$ but there is a strong general tendency for the absorbing gas to avoid $\Delta l = 0''$, $\Delta b = 0''$. This tendency has been recognized for some time, but cannot be explained, as was sometimes done earlier, as an artifact of geometry with most gas passing behind (West). As shown in Sect. IV, the ^{12}CO gas column density is well traced by the H I absorption data.

IV. Comparison of H I absorption and emission

It is important to discern between variations in apparent line opacity due to geometry and those due to spatial structure in the H I gas density or spin temperature. One way to accomplish this is to compare absorption and emission spectra, but H I emission

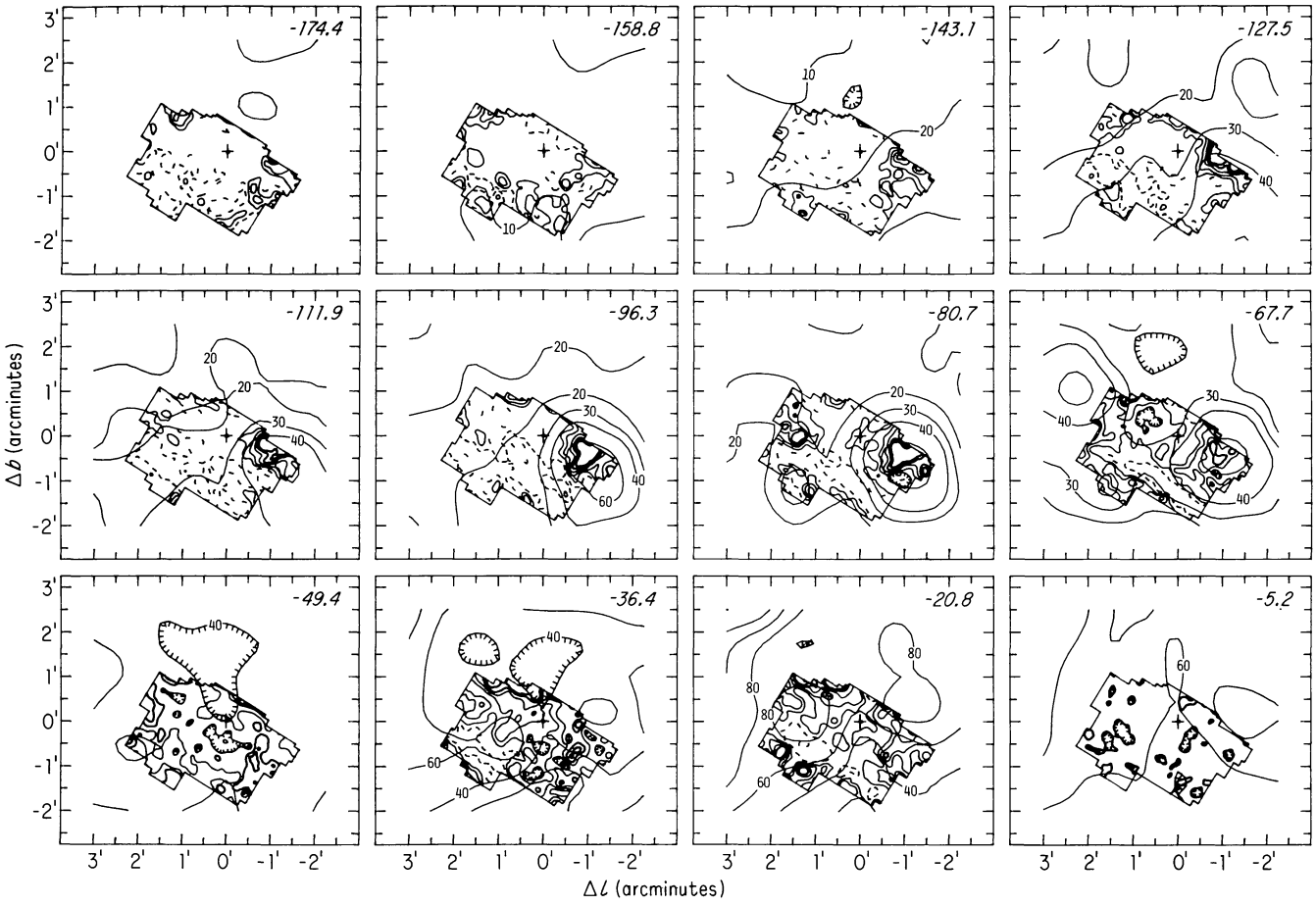

Fig. 4. Comparison of integrated H I opacity and ^{12}CO radiation temperature $T_r \equiv T_A^*/0.65$ at λ2.6 mm. Labelled contours (units K km s^{-1}) are for ^{12}CO, taken with a $\sim$66″ beam at 45″ spacings; contours within the irregularly shaped boundary are $\int \tau dv$ as in Fig. 2. The range of integration is $\approx$15 km s^{-1} about the center velocity indicated. These maps show that column density variations determine the H I optical depth patterns. If the H I gas fraction is approximately constant ($\sim$1%) it follows (see Sect. IV) that $\tau \propto T_r$

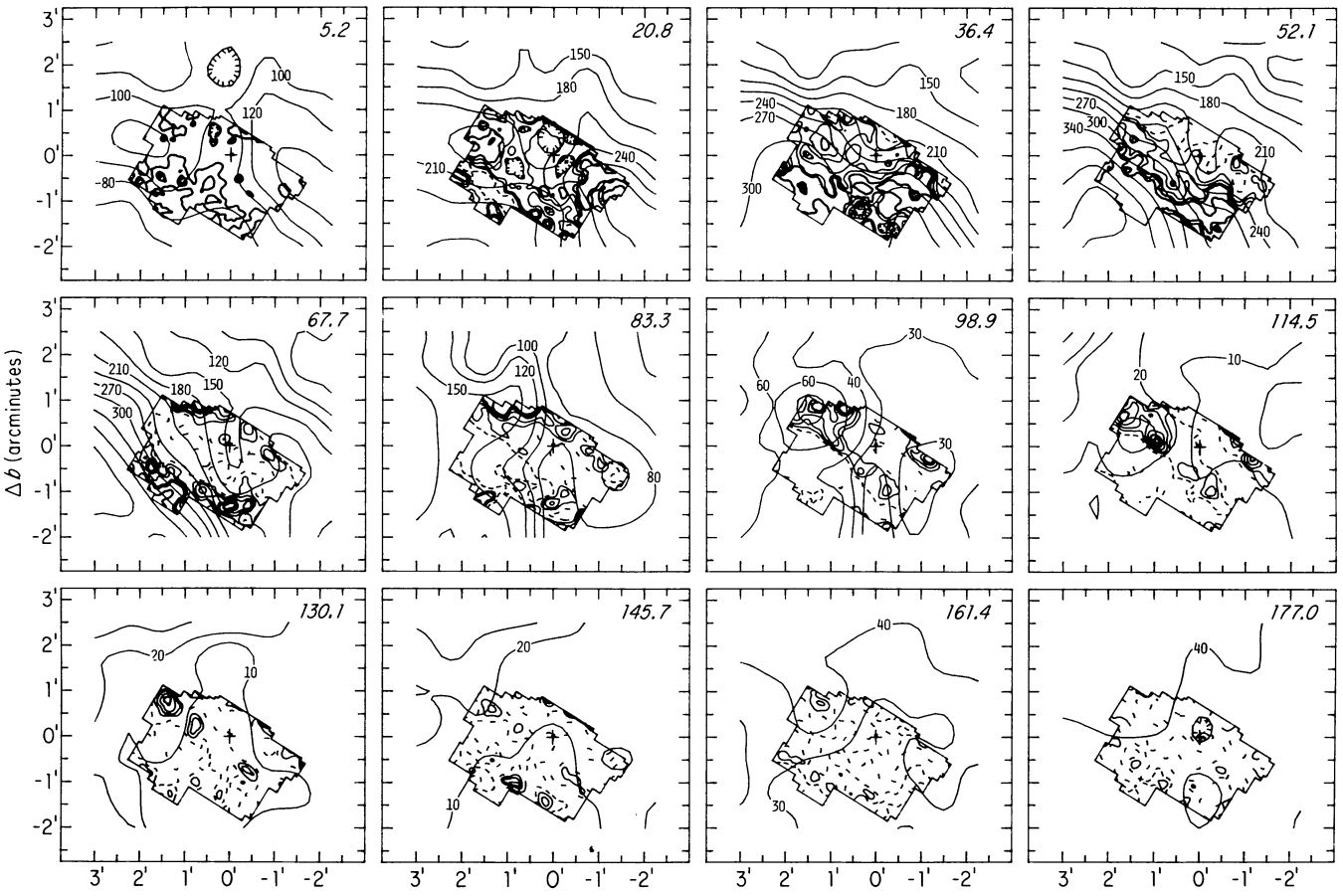

Fig. 4 (continued)

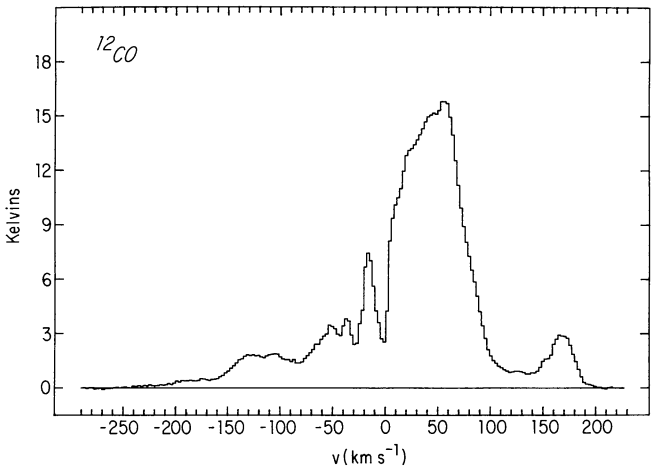

Fig. 5. The average ^{12}CO emission spectrum over the region mapped in Fig. 4. H I absorption is seen over most of the range prominent in emission, i.e. at $-200\,\mathrm{km\,s^{-1}} \leqq v \leqq 140\,\mathrm{km\,s^{-1}}$

spectra of this region are not obtainably with sufficient detail. We decided to approach this problem by testing if the correlations between H_2CO absorption and CO emission found earlier also pertained for the case of the nuclear H I. Earlier work has shown that H I *self*-absorption features generally have CO emission counterparts (Burton et al., 1978; Liszt et al., 1981) and that the ^{12}CO emission intensities are well correlated with column densities for features seen over large regions around the galactic nucleus (Liszt and Burton, 1979). The CO data taken for the purpose of this test show that, with a few minor exceptions, there is a striking correlation of CO intensity and H I opacity measured toward Sgr A. This result allows us to establish that the structures appearing in H I absorption form patterns which can be traced on a larger scale in CO emission, and also allows geometry/opacity ambiguities to be addressed.

Shown in Fig. 4 are maps representing ^{12}CO line intensity integrals taken over six channels ($15.6\,\mathrm{km\,s^{-1}}$) and spaced six channels from panel to panel. H I optical depths integrated over three channels ($15.5\,\mathrm{km\,s^{-1}}$) and spaced by three channels have been overlaid with these data. The center velocity shown is that of the ^{12}CO: to track the H I data more precisely the CO map separation is occasionally 5 channels, but the H I and CO data have center velocities within $1.2\,\mathrm{km\,s^{-1}}$ in all cases.

The broad negative-velocity feature in ^{12}CO at $\Delta l \sim -1'$ is clearly localized in emission around the H I peak. At negative velocities $v \geqq -60\,\mathrm{km\,s^{-1}}$ the CO-H I correlation is less well-defined because the ^{12}CO is self-absorbed or only weakly emitting. The average of all the ^{12}CO spectra shows dip at $\sim -45\,\mathrm{km\,s^{-1}}$, $-30\,\mathrm{km\,s^{-1}}$, and $0\,\mathrm{km\,s^{-1}}$ (Fig. 5). The "line" at $\sim -17\,\mathrm{km\,s^{-1}}$ is an artifact of the latter two absorptions.

At positive velocities $v \sim 20\,\mathrm{km\,s^{-1}}$ in Fig. 4 the twin peaks on either side of (West) have the structure noted earlier in H_2CO synthesis (Whiteoak et al., 1974) and in ^{12}CO emission (Liszt et al., 1975): the H I and molecular gases are well mixed. At 30–60 $\mathrm{km\,s^{-1}}$ the very strong spatial gradient in H I opacity from

Sgr A (East) to (West) is present in ^{12}CO emission as well, providing additional evidence that it is a column density effect. At least up to $v\sim+120\,km\,s^{-1}$ the H I peaks occur in regions of enhanced ^{12}CO intensity.

The great majority of the H I apparent optical depth variations can be readily associated with column density variations if it is accepted that the H I and CO (or H_2CO) are well mixed, with H I opacity arising from a residue of cold H I in molecular material. The actual H I gas fraction is probably roughly constant for any one feature. Simple estimates of the CO column density, made by comparing ^{12}CO and ^{13}CO observations, using $T_k\approx T_b(^{12}CO)$, vary roughly as $T_b^2(^{12}CO)$ if the $^{12}CO/^{13}CO$ intensity ratio is approximately constant. If the H I spin temperature $T_{spin}\sim T_b$, it follows that the H I opacity would track $T_b(^{12}CO)$ if the H I/CO abundance ratio is fixed ($\tau_{HI}\propto N_{HI}/T_{spin}\propto N_{CO}/T_b\propto T_r^2/T_b=T_b$). Comparing the -80 and $+50\,km\,s^{-1}$ line integrals of H I and CO and using the locally determined ratio $N_H/\int T_A^* dv\sim 1\pm0.5\,10^{21}\,cm^{-2}$ $(K\,km\,s^{-1})^{-1}$ (Liszt, 1982), one finds $N_{HI}/N_{H_2}\sim0.01$ at both velocities. Similar values are also required for H I self-absorption in the galactic plane at higher longitudes (Liszt et al., 1981).

Sandqvist (1982) has used a comparison of $\lambda\,6\,cm\,H_2CO$ absorption and $\lambda\,2\,mm\,H_2CO$ emission in the manner discussed here. By varying the combinations whereby (East) and (West) may each lie on either side of the molecular gas, he determines the source-gas geometry by demanding similarity of the spatial morphology at the two wavelengths (i.e. he computes the $\lambda\,6\,cm$ optical depth for each combination using the known continuum structure and assuming a uniform, more distant continuum background). His conclusion, that Sgr A (East) lies in front of the gas and (West) behind it, is inconsistent with the appearence of saturated lines toward (East) in the H I data (see also Schwarz et al., 1982) and in the H_2CO synthesis unless it is assumed that most of the flux detected toward (East) arises behind it. Because this seems unlikely, and because both (East) and the compact source are occulted by the same gas, all of Sgr A must lie behind the gas cloud.

V. High-negative-velocity gas

The ^{12}CO profile in Fig. 5 shows emission at low levels out to $\sim-240\,km\,s^{-1}$. At $-190\,km\,s^{-1}$ there occurs a feature first observed by Güsten and Downes (1981) using 9′ resolution H I and 2.′7 resolution H_2CO data. This feature is also visible in Fig. 1 at $\Delta l\sim-30''$. This gas is too weak to map in the H I absorption but its distribution in ^{12}CO is shown in a series of maps in Fig. 6. The feature is strongest in a vertical ridge at $\Delta l\sim-45''$ which is not well resolved at 60″ resolution, but extends over $>180''$ in Δb and more weakly to $\Delta l>0''$. Although our observations do not strongly support the argument of Güsten and Downes (1980) that rotation is ruled out because the feature occurs at both positive and negative Δl, there is also no evidence of the expected rotational velocity gradient (this gas appears most prominently in a constant-longitude at $\Delta l<0''$). Higher spatial-resolution maps are clearly required. We note that the masses and densities inferred by Güsten and Downes, $M>10^3\,M_0$, $n_{H_2}\geqq10^3\,cm^{-3}$, are consistent with the ^{12}CO data.

VI. Discussion and summary

The H I absorption patterns observed toward Sgr A are only very fragmentary images of the general gas distribution: most of the features which can be discerned extend over larger angular scales than that of the continuum complex itself ($\sim180''$ or ~9 pc) and only a few have any possibility of lying sufficiently near the galactic nucleus that their physical properites are strongly affected by its presence. Accordingly, we limit our comments here mainly to the intermediate positive-velocity gas most directly associated with Sgr A. We note in passing that our data do not lead us to a discussion of ejected phenomena.

One of the more striking characteristics of the H I absorption is the annular nature of the total optical depth maps in Fig. 3, a pattern which is found as well in ^{12}CO emission, in H_2CO absorption, and at infrared wavelengths long enough to sample dust in the gas clouds (Gatley, 1982). If, as has been claimed (Güsten and Downes, 1980) the inner 100 pc (projected angular extent $\pm15'$) is free of neutral gas, this small-scale structure centered on the continuum complex is purely accidental. However, there is evidence that Sgr A is closely associated and interacting with molecular material: CO emission at 40–$70\,km\,s^{-1}$ shows a strong peak just outside the eastern boundary of (East). Although it is unusual for hot ($T_b>20\,k$) CO emission to occur near a non-thermal source, the recent detection of two compact H II regions at this position by Ekers et al. (1982) leads us to believe that compression of the molecular material and star formation within it have occurred. Infrared observations (Gatley, 1982; Rieke, 1982) show that the central 1 pc of the Galaxy is relatively free of dust and it seems reasonable to associate this with the absorption patterns also indicating an absence of high-density neutral material in the same direction. Both the non-thermal shell structure and the central void may have been caused by a recent supernova (10^3–10^4 yr ago) whose remnant is now bounded by the remaining dense ambient gas. In this case, a large part of the decrease in absorbing column density toward Sgr A (West) would not result solely from a fortuitous geometry. Rieke (1982) has cited the apparent lack of dense gas in the innermost regions of the Galaxy as a mild contradiction to the last (10^6 yr ago), highly productive round of star formation there. Although, however, there is no dense neutral gas in the innermost 5 pc of the Galaxy, radio continuum (Ekers et al., 1983) and 2 cm radio recombination line observations (Bregman and Schwarz, 1982; van Gorkom et al., 1983) indicate that dense ionized gas does exist there. A comparison between our H I/CO data and the recombination line observations indicates that the neutral and ionized material match remarkably at $-100\,km\,s^{-1}$ at $\Delta l\sim-60''$ and at $+100\,km\,s^{-1}$ at $\Delta l\sim+60''$ in the sense that material at larger projected angular separation is neutral whereas material closer to the galactic center but at the same velocity is ionized. This suggests that gas within 60″ or 3 pc from the galactic center has become ionized by some mechanism (shocks or radiation). Whether this gas has been pushed toward the center by the supernova, of which we think (East) is the relic, or whether there is another explanation is presently unclear. A detailed interpretation of this remarkable fact must await the final results from the recombination line observations by van Gorkom et al. (1983).

The origin of the positive-velocity gas toward Sgr A has been the subject of much discussion. That part (or even most of this gas) shows a large velocity gradient, as evident in Fig. 4, has been interpreted as an individual rotating cloud (Sandqvist, 1970); this gas is, nevertheless, contained in a large structure seen fairly continuously at $\Delta b=0''$ over the range $-220\,km\,s^{-1}\leqq v\leqq100\,km\,s^{-1}$, $-120'\leqq\Delta l\leqq30'$ (see Fig. 1 of Liszt and Burton, 1978). Except for the fact that it crosses $v=0\,km\,s^{-1}$ at $\Delta l\lesssim-5'$, the kinematic signature of this feature in the position-velocity plane indicates a simple origin of pure rotational motion. The higher-velocity features at $v\sim90$–$135\,km\,s^{-1}$ also arise as part of a

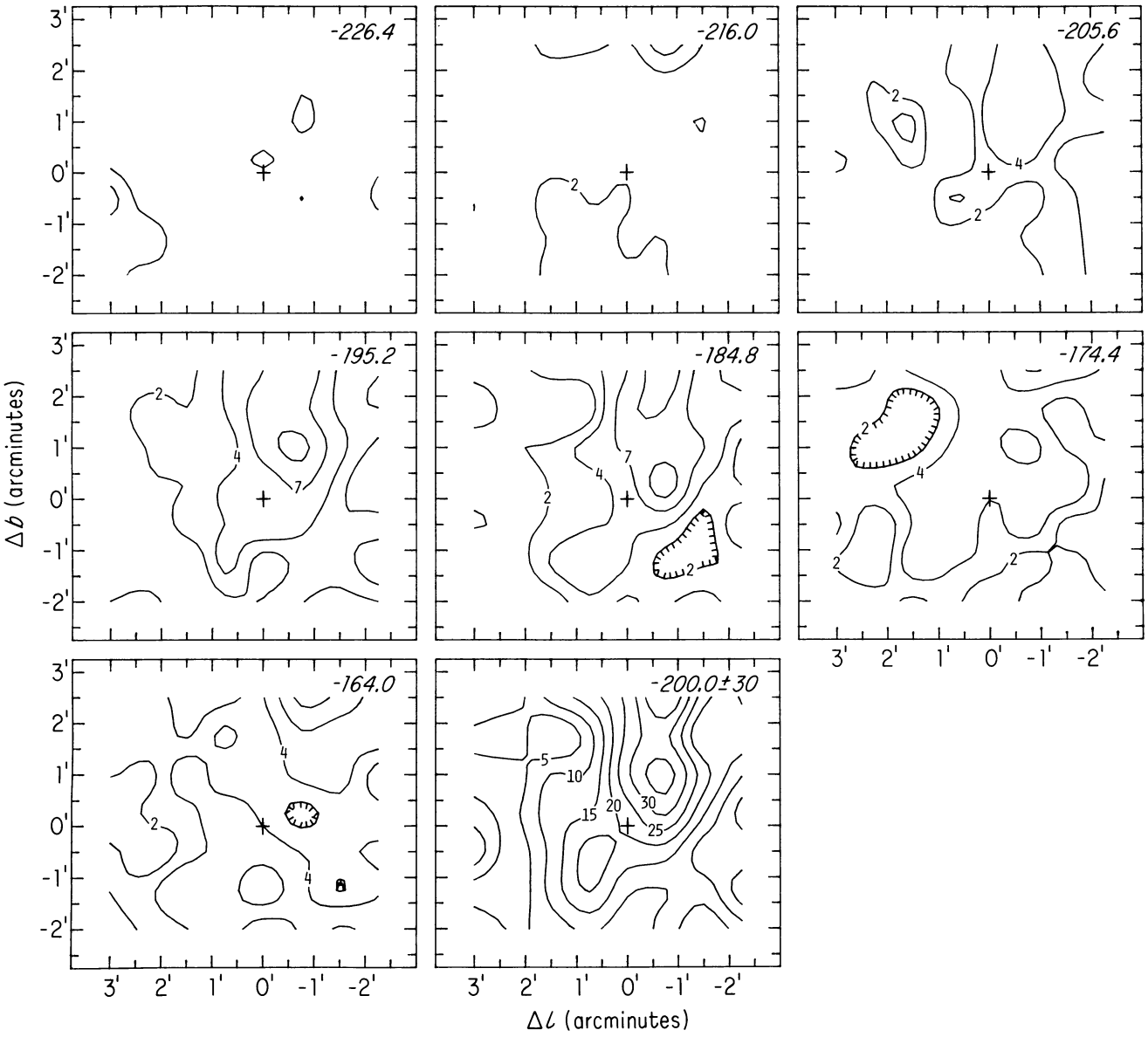

Fig. 6. Maps of integrated ^{12}CO radiation temperature at high negative velocities. The velocity range of integration is 10 km s^{-1} about the velocity indicated except for the bottom right panel. This gas occurs mainly in a ridge at $l = -0.5$ which is not spatially resolved in longitude

(broad-lined) extended structure showing a strong rotational velocity gradient in ^{12}CO emission, but this second feature crosses the longitude of Sgr A at even higher velocity 80–90 km s^{-1} and at positive latitudes. It is unclear how these two are related. We hope to present a unified description in forthcoming discussions of our finely sampled survey of ^{12}CO emission over the range $-35' \leqq \Delta l \leqq 50'$ (Liszt and Burton, 1983, in preparation).

We summarize this work as follows:

1. H I absorption patterns toward Sgr A are controlled by column density variations in intervening molecular clouds. The absorptions, except perhaps in a few features (like the 3 kpc arm or the 0 velocity feature) occur because a small fraction ($\sim$1%) of the H content remains atomic. Few of the absorption features arise in warm, "diffuse" atomic clouds.

2. The extended, non-thermal radio continuum source may be physically bounded by ambient molecular material.

3. The region of Sgr A (West) around (or toward) the compact source is occulted by gas at 40–70 km s^{-1} which is part of the feature strongly seen in absorption against Sgr A (East). The most plausible geometry consistent with observations places both continuum components behind this positive-velocity gas.

4. H I absorption features are found over the entire range -200 km s$^{-1} \lesssim v \lesssim 140$ km s^{-1}; ^{12}CO emission extends to $\sim +200$ km s^{-1}. Gas at most of the velocity range visible in emission lies between the Sun and Sgr A.

5. Gas at -190 km s^{-1} lies mainly in a thin structure, extending several arcminutes in Δb at $\Delta l \sim -45''$.

Acknowledgements. We are grateful to J. H. van Gorkom, U. J. Schwarz and J. D. Bregman for permission to quote their unpublished VLA recombination line data. The U.S. National Science Foundation supported some of this work at the

University of Minnesota through grant AST-7921812 to W.B.B. and grant AST-7922024 to J.M. v.d. H.. H.S.L. and W.B.B. gratefully acknowledge support from the North Atlantic Treaty Organization through Research Grant No. 008.82. The National Radio Astronomy Observatory is operated by Associated Universities, Inc., under contract with the National Science Foundation. The Netherlands Foundation for Radio Astronomy (S.R.Z.M.) is supported by the Netherlands Organization for the Advancement of Pure Research (Z.W.O.).

References

Bregman, J.D., Schwarz, U.J.: 1982, *Astron. Astrophys.* **112**, L 6
Brown, R.L., Johnston, K.J., Lo, K.Y.: 1981, *Astrophys. J.* **250**, 155
Burton, W.B., Liszt, H.S., Baker, P.L.: 1980, *Astrophys. J. Letters* **219**, L 67
Ekers, R.D., van Gorkom, J., Schwarz, U., Goss, W.M.: 1983, *Astron. Astrophys.* (in press)
Gatley, I.: 1982, in *The Galactic Center*, eds. G.R. Riegler and R.D. Blandford, p. 25
Güsten, R., Downes, D.: 1980, *Astron. Astrophys.* **87**, 6
Güsten, R., Downes, D.: 1981, *Astron. Astrophys.* **99**, 27
Kerr, F.J., Westerhout, G.: 1965, in *Stars and Stellar Systems*, eds. A. Blaauw and M. Schmidt, V, p. 167
Lacy, J.H., Baas, F., Townes, C.H., Geballe, T.R.: 1979, *Astrophys. J. Letters* **27**, L 17
Lacy, J.H., Townes, C.H., Geballe, T.R., Hollenbach, D.J.: 1980, *Astrophys. J.* **241**, 132
Linke, R.A., Stark, A.A., Frerking, M.A.: 1981, *Astrophys. J.* **243**, 147
Liszt, H.S.: 1982, *Astrophys. J. Letters* (in press)
Liszt, H.S., Burton, W.B.: 1978, *Astrophys. J.* **226**, 790
Liszt, H.S., Burton, W.B.: 1979, *Astrophys. J.* **228**, 105
Liszt, H.S., Burton, W.B., Bania, T.M.: 1981, *Astrophys. J.* **246**, 74
Liszt, H.S., Sanders, R.H., Burton, W.B.: 1975, *Astrophys. J.* **198**, 537
Menon, T.K., Ciotti, J.E.: 1970, *Nature* **227**, 579
Rieke, G.H.: 1982, in *The Galactic Center*, eds. G.R. Riegler and R.D. Blandford, p. 25
Rougoor, G.W.: 1964, *Bull. Astron. Inst. Neth.* **17**, 381
Rougoor, G.W., Oort, J.H.: 1960, *Proc. Natl. Acad. Sci.* **46**, 1
Sandqvist, Aa.: 1970, *Astron. J.* **75**, 135
Sandqvist, Aa.: 1982, in *The Galactic Center*, eds. G.R. Riegler and R.D. Blandford, p. 12
Schwab, F.: 1980, *Proc. S.P.I.E.* **231**, 18
Schwarz, U., Ekers, R.D., Goss, W.M.: 1982, *Astron. Astrophys.* **110**, 100
Scoville, N.Z.: 1972, *Astrophys. J. Letters* **175**, L 127
Thompson, A.R., Clark, B.G., Wade, C.M., Napier, P.J.: 1980, *Astrophys. J. Suppl.* **44**, 51
van Gorkom, J., Schwarz, U.J., Bregman, J.D.: 1983 (in preparation)
van Woerden, H., Rougoor, W.N., Oort, J.H.: 1957, *C.R.* **244**, 1691
Whiteoak, J.B., Rogstad, D.H., Lockhart, I.A.: 1974, *Astron. Astrophys.* **36**, 245